A Novel Transmitter Architecture for Combined Baseband Data and Subcarrier-Multiplexed Control Links Using Differential Mach–Zehnder External Modulators

R. Gaudino and D. J. Blumenthal, *Member, IEEE*

***Abstract*—We propose, analyze, and demonstrate a novel transmitter architecture for links that support transmission of baseband data and subcarrier multiplexed control channels. The architecture utilizes a differential external integrated-optic modulator to electrooptically combine the baseband and subcarrier multiplexed data onto an optical carrier. An analytical model is presented that allows optimization of the SNR of the received baseband and control data channels based on modulation parameters. This optimization is based on tradeoffs that result when the baseband and subcarrier channel are combined using a nonlinear modulator transfer function. We experimentally demonstrate a link based on this architecture with 2.5-Gb/s baseband and 100-Mb/s control data multiplexed on a 5.5-GHz subcarrier. Analytical and measured experimental results are compared and are shown to be in good agreement.**

***Index Terms*—Optical communication, optical modulation, optical networks, subcarrier multiplexing.**

I. Introduction

OPTICAL subcarrier multiplexing (OSCM) has been proposed and demonstrated as an efficient solution to delivering digital control information over optical and all-optical wavelength-division multiplexed (WDM) networks [1]–[5]. In these systems, a subcarrier multiplexed signal is transmitted with a baseband signal on each wavelength. Subcarrier-multiplexed (SCM) detection can be performed by simple photodetection, followed by microwave bandpass filtering, without baseband bit-rate syncronization. It is expected that baseband rates in excess of 10 Gb/s and control channels on the order of several hundreds of Mb/s must be supported with subcarrier frequencies that lie outside the baseband channel. Previously reported work [3], [4] combined baseband and subcarrier signals at the electronic level followed by direct laser modulation. In this letter, we analyze a transmitter architecture that combines the baseband and subcarrier signals electrooptically based on a differentially driven external integrated-optic modulator. This approach does not require an electronic, dc-coupled summing circuit, that introduces excess resistive losses in the electronic driving circuits.

An analytical model is developed to specify transmitter operating parameters for optimal baseband and subcarrier channel performance. The model takes into account the modulator nonlinear transfer function and several parameters such as payload and SCM control channel driving amplitudes and bias voltages. Reslts from an experimental link that supports 2.5-Gb/s baseband and 100-Mb/s control channel multiplexed on a 5.5-GHz subcarrier is demonstrated and compared to the analytical results.

Manuscript received February 14, 1997; revised June 12, 1997. This work was supported by the National Science Foundation under a National Young Investigator Award 94-57148 and by the Associazione Elettrotecnica Italiana.

R. Gaudino is with the Dipartimento di Elettronica, Politecnico di Torino, Torino, Italy. He is also with the Optical Communications and Photonic Networks Group, Microelectronics Research Center, School of Electrical and Computer Engineering, Georgia Institute of Technology, Atlanta, GA 30332-0250 USA.

D. J. Blumenthal is with the Optical Communications and Photonic Networks Group, Microelectronics Research Center, School of Electrical and Computer Engineering, Georgia Institute of Technology, Atlanta, GA 30332-0250 USA.

Publisher Item Identifier S 1041-1135(97)07174-7.

II. Transmitter Architecture

The link architecture is shown in Fig. 1. A digital baseband signal and a digitally modulated microwave subcarrier are separately generated, then combined using two differential arms of an external modulator. The transmitter may be based on one of several types of external multiarm modulators with differential electrical ports (e.g., Mach–Zehnder (MZ), $\Delta\beta$ couplers, etc.). The transfer function must be expressable as

$$P_{\text{out}} = P_0 f(V_1 - V_2) \tag{1}$$

where P_{out} is the optical output power, V_1, V_2 are the two applied voltages, P_0 is a reference power, and f is a generic (usually nonlinear) function. A baseband (V_1) and a microwave subcarrier modulated signal (V_2) are applied separately to the two arms of the modulator, as shown in the left side of Fig. 1.

III. Analysis

Assuming that signals $V_1(t)$, $V_2(t)$ and bias voltage $V_{\text{bias},1}$ are applied to the two arms of a MZ modulator. The output optical power can be expressed as

$$P_{\text{out}}(t) = P_o \cos^2\left\{\frac{[V_1(t) + V_{\text{bias},1}] - V_2(t)}{V_\pi}\right\} \tag{2}$$

where $P_o = P_{\text{in}}L$, L is the total MZ loss, P_{in} is the optical input power, and V_π is the switching voltage. We introduce the following notation for the baseband, control, and bias signal:

$$\begin{aligned} V_{\text{base}}(t) &= V_1(t) = aV_\pi\alpha(t) \\ V_{\text{cont}}(t) &= V_2(t) = -bV_\pi\beta(t)\cos(2\pi f_s t + \phi) \\ V_{\text{bias}} &= V_{\text{bias},1} = V_\pi c \end{aligned} \tag{3}$$

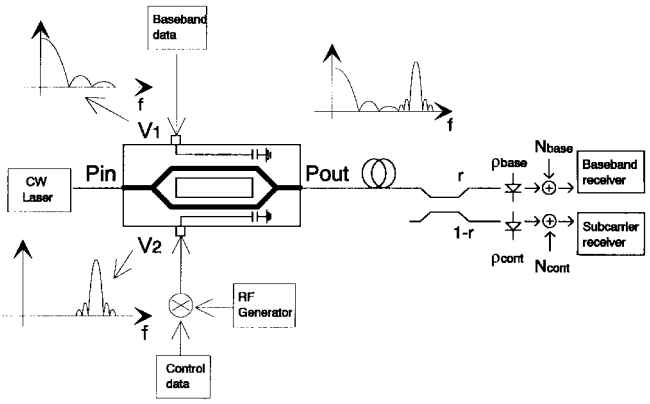

Fig. 1. Schematic of our OSCM architecture based on differential external modulator, together with a schematic of a generic baseband and subcarrier receiver.

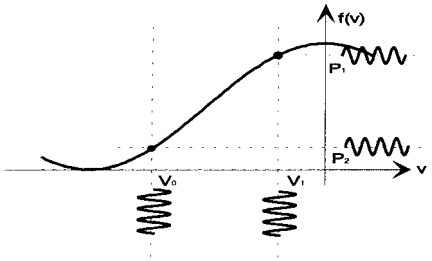

Fig. 2. Nonlinear mapping of payload and header modulation by Mach–Zehnder interferometric modulator illustrates operating end points for baseband data and binary quiescent operating points for subcarrier multiplexed control channel.

where $\alpha(t) = 0, 1$ is the baseband data at bit rate $B_{\text{base}} = 1/T_{\text{base}}$, $\beta(t) = 0, 1$ is the control channel data at bit rate $B_{\text{cont}} = 1/T_{\text{cont}}$, and the subcarrier is defined by its frequency f_s and constant phase ϕ.

In (3), we have normalized the signal amplitudes to the modulator V_π voltage. The following optimization is based on the parameters a, b, c, which are, respectively, the baseband, control, and bias amplitude, normalized to V_π. The output power is written as

$$P_{\text{out}} = P_o \cos^2 [a\alpha(t) + b\beta(t) \cos(2\pi f_s t + \phi) + c]. \quad (4)$$

We assume on–off keying (OOK) modulation on baseband and control channels. Other modulation techniques (PSK, FSK) for the control channel can be easily taken into account by choosing different values for β and letting ϕ change at the control channel bit rate.

The relationship between the modulator transfer function and the baseband and OSCM control signals is illustrated in Fig. 2. The baseband data set large-signal quiescent operating points about which the relatively smaller subcarrier signal is modulated. This relationship illustrates the compromise between baseband and control data performance. In order to increase baseband performance, the on–off operating points should be separated as far as possible placing the quiescent points at the maximum and minimum of the modulator transfer function. However, these operating points produce maximum nonlinear distortion of the subcarrier channel, reducing the overall control channel amplitude and increasing interference between the baseband and subcarrier channel due to intermodulation distortion. An optimum operating condition will specify the point at which both the baseband excursion and subcarrier signal strength can be simultaneously maximized.

Expanding (4) in a Taylor series around $b \to 0$, we obtain

$$\begin{aligned}\frac{P_{\text{out}}(t)}{P_o} \simeq\ & f[a\alpha(t)+c] + f_1[a\alpha(t)+c]b\beta(t)\cos(2\pi f_s t+\phi) \\ & + \tfrac{1}{4} f_2[a\alpha(t)+c]b^2\beta(t) \\ & + \tfrac{1}{8} f_3[a\alpha(t)+c]b^3\beta(t)\cos(2\pi f_s t+\phi) \quad (5)\end{aligned}$$

where $f(x) = \cos^2(x)$ and its ith-order derivatives f_i.

The first two terms are the useful baseband and control data output components. The last two terms account for nonlinear beating between baseband and control data around $f = 0$ and $f = f_s$, respectively. The useful baseband term $f[a\alpha(t)+c]$ is dependent on the bias c and on the baseband input amplitude a only, as would be in the absence of the subcarrier signal. The useful control channel term $f_1[a\alpha(t)+c]b\beta(t)\cos(2\pi f_s t+\phi)$ does not depend on b only, but on a and c as well and is consequently affected by the values chosen for the baseband and bias amplitudes.

Introducing the baseband operating points $V_1 = (a+c)V_\pi$ and $V_0 = cV_\pi$ corresponding to the transmission of a "1" or a "0" bit, the output baseband levels can be expressed as $P_1 = P_o f(V_1)$, $P_0 = P_o f(V_0)$. The control data have an instantaneous power oscillating around P_1 or P_0 with a peak-to-peak swing varying between $P_o f_1(V_1)\, b$ and $P_o f_1(V_0)\, b$ at the payload rate.

We restrict our attention to the case in which the driving voltage is in the range $[-V_\pi, 0]$ (any other choice $[(n-1)V_\pi, nV_\pi]$ would lead to identical results). If no control data are present, the optimal choice is ideally $V_0 = -V_\pi$ and $V_1 = 0$ (corresponding to $a = 1$, $c = -1$) which gives $P_1 = P_{\text{out}}$ and $P_0 = 0$. Under these circumstances, $f_1(V_0) = f_1(V_1) = 0$. For control data alone, the optimum point is the one that maximizes f_1, i.e., $V_0 = V_1 = -V_\pi/2$.

We analyze the simplified model shown in Fig. 1 that corresponds to a system limited by electrical receiver noise, as in the experiment described in the following section. Here, r is the splitting ratio of the optical coupler and ρ_{base} and ρ_{cont} are the responsivities of the photodiodes and N_{base}, N_{cont} the power spectral densities of the two receiver equivalent noise sources. The filters and envelope detectors are assumed to be ideal (integrate and dump filters) in order to obtain an analytical expression for the received Q value, where $Q = (m_1 - m_0)/(\sigma_1 + \sigma_0)$. The parameters, m_1 and m_0, are the mean values of the noisy decision signal at the sampling instant, when a "1" or a "0" are transmitted, respectively, and σ_1, σ_0 are the corresponding standard deviations. The value $Q = 6$ corresponds approximatively to a bit error rate equal to 10^{-9}. Following the steps outlined in [6], the received Q values can be written as

$$\begin{aligned}Q_{\text{base}} &= \frac{r\rho_{\text{base}} P_{rx} A_{\text{base}}}{\sqrt{2N_{\text{base}}B_{\text{base}}}} \\ Q_{\text{cont}} &= \frac{(1-r)\rho_{\text{cont}} P_{rx} A_{\text{cont}}}{\sqrt{2N_{\text{base}}B_{\text{cont}}}} \quad (6)\end{aligned}$$

where $P_{rx} = L_{\text{link}} P_o$ and L_{link} is the total link loss. A_{base} is the normalized output baseband swing [$A_{\text{base}} = f_0(a+c) -$

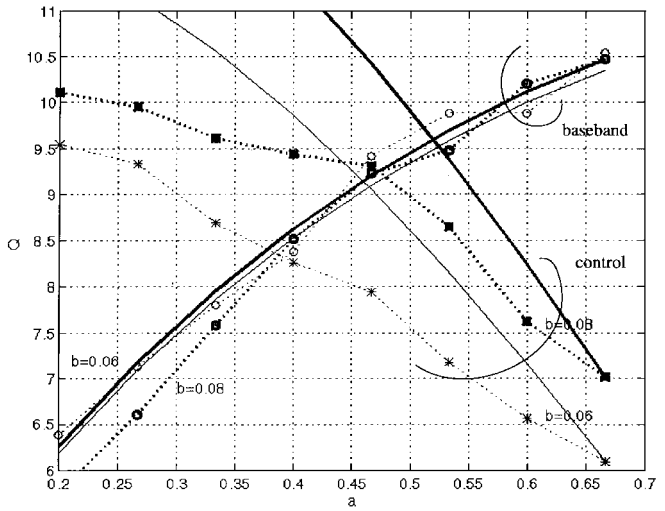

Fig. 3. Experimental (point and dashed lines) and analytical (solid lines) measurement of Q_p and Q_h as a function of the normalized baseband signal amplitude a for two different values of the normalized control signal amplitude b.

$f_0(c)$ when $b = 0$] and $A_{\rm cont}$ is the average normalized output control data amplitude.

$A_{\rm base}$ and $A_{\rm cont}$ can be expressed as

$$A_{\rm base} = f_0(a+c) - f_0(c) + \frac{b^2}{4}\left[f_2(a+c) - f_2(c)\right]$$

$$A_{\rm cont} = \frac{1}{2}\left[f_1(a+c) + f_1(c)\right] + \frac{b^3}{16}\left[f_3(a+c) + f_3(c)\right] \quad (7)$$

assuming $T_{\rm cont} \gg T_{\rm base}$, so that the baseband-rate oscillating term $f_1[a\alpha(t)+c]$ on the control data signal can be averaged and interchannel interference neglected. Using (6) and (7), $Q_{\rm base}$ and $Q_{\rm cont}$ are expressed as functions of a, b, c and can be optimized to obtain the highest $Q_{\rm base}$ under the assumption $Q_{\rm base} = Q_{\rm cont}$, corresponding to the same bit-error rate (BER) on both signals. This constraint may be adjusted based in the specific architecture and performance needs.

IV. Experimental Results and Comparison to Theory

An experimental transmitter architecture was to test our model. We set up a link with a 2.5-Gb/s OOK baseband signal and a 100-Mb/s OOK digitally modulated 5.5-GHz subcarrier experimentally applied to independent arms of a differentially driven $LiNbO_3$ MZ modulator, with demonstrated $V_\pi = 3.0$ V and a 3-dB modulation bandwidth equal to 6 GHz.

At the receiver, the signal was split to the baseband and OSCM branches using a 4:1 splitting ratio with the received optical powers measured to be $P_{\rm base} = -10.4$ dBm and $P_{\rm cont} = -16.4$ dBm. The baseband signal is photodetected and filtered and the resulting Q value was measured. The control data were detected by following a photodiode with a traveling-wave amplifier and a bandpass filter with center frequency of 5.5 GHz and 3-dB bandwidth $f_{3\,\rm dB} = 500$ MHz. The electronic subcarrier signal is further amplified and incoherently detected using a Schottky diode followed by a low-pass filter with corner frequency $f_{3\,\rm dB} = 100$ MHz. We measured the baseband and control signal-to-noise-ratio (SNR) values $Q_{\rm base}$ and $Q_{\rm cont}$ as a function of the modulator input voltages $V_{\rm base}$, $V_{\rm cont}$, $V_{\rm bias}$.

In Fig. 3, we show the results as a function of $a = V_{\rm base}/V_\pi$ and $b = V_{\rm cont}/V_\pi$ for two different values of $V_{\rm cont}$ corresponding to measured values of $b = 0.08$ and $b = 0.06$. The bias voltage $V_{\rm bias}$ was set to obtain the best performances for each point. The baseband Q is strongly dependent on a, while the dependence on b is negligible and is obscured by measurement errors. However, control data performances are strongly affected by both a and b. Assuming that the target is to obtain $Q_{\rm base} = Q_{\rm cont}$, the choice $a = 0.45$, $b = 0.08$ leads to $Q_{\rm base} = Q_{\rm cont} \simeq 9.3$.

In the same figure, we report the results obtained using the analytical formulation (solid lines). The predicted and experimental results are qualitatively similar illustrating that optimal BER conditions can be achieved for the baseband and control channels as indicated by the intersection of the baseband and control data curves. Differences between analytical and experimental results are due to nonideal filtering, nonideal response of the Schottky diode and interchannel interference. This last effect has greater impact on the control signal, due to its lower spectral power relative to the baseband.

We also found that the performances on the subcarrier signal are strongly dependent on the bias voltage. The optimum value is the one which sets the two baseband operating points symmetrically with respect to the center of the transfer function ($-V_\pi/2$ using our conventions). In our setup, a 10% accuracy around this optimal point was required to limit performance degradation on the control channel to less than 1 dB.

V. Conclusion

We have experimentally demonstrated a novel configuration for baseband and OSCM transmission using a differentially driven MZ external modulator. The transmitter optoelectronically combines baseband and control signals. We have developed an analytical tool that allows us to model the effects of the MZ nonlinear transfer function and to optimize link performance by properly choosing transmitter operating points. Experimental and analytical SNR for both baseband and control signals have been compared and shown to be in good agreement. Future work will involve modeling and demonstration of this architecture with other differentially driven external modulators ($\Delta\beta$ coupler, electroabsorption, etc.).

References

[1] A. Budman, E. Eichen, J. Schlafer, R. Olshansky, and F. McAleavey, "Multigigabit optical packet switch for self-routing networks with subcarrier addressing," in *Conf. Optical Fibers and Communications*, San Jose, CA, Feb. 1992, pp. 90–91.

[2] Special issue on Multiwavelength optical technology and networks, *J. Lightwave Technol.*, vol. 14, June 1996.

[3] E. Park and A. E. Willner, "Network demonstration of self-routing wavelength packets using an all-optical shifter and QPSK subcarrier routing control," in *Proc. OFC'96*, San Jose, CA, 1996.

[4] M. Cerisola, M. Fong, T. K. Hofmeister, R. T. Kazovsky, L. G. Lu, C. L. Poggiolini, and P. Sabido, "CORD—A WDM optical network: Control mechanism using subcarrier multiplexing and novel synchronization solutions," in *IEEE Int. Conf. Communications*, Piscataway, NJ, 1995, pp. 261–265.

[5] M. Shell, M. D. Vaughn, A. Wang, D. J. Blumenthal, P. J. Rigole, and S. Nilsson, " Experimental demonstration of an all-optical routing node for multi-hop wavelength routed networks," *IEEE Photon. Technol. Lett.*, vol. 8, pp. 1391–1393, Oct. 1996.

[6] P. Poggiolini and S. Benedetto, "Theory of subcarrier encoding of packets header in quasiall-optical networks," *J. Lightwave Technol.*, vol. 12, pp. 1869–1881, June 1994.